Optical Frequency Domain Differential Phase Shift Keying in Femtosecond-Pulse Spectral Modulation Systems

June-Koo Rhee, Hisashi Kobayashi, *Fellow, IEEE,* and Warren S. Warren

***Abstract*— We propose a novel scheme of differential phase shift keying (DPSK) in the optical frequency domain. We take advantage of the intrinsic coherence among spectral elements derived by spectrum slicing a femtosecond optical pulse, introducing differential phase modulation between adjacent spectral elements with a femtosecond-pulse shaper. Detection of the differential phase is achieved by a Mach–Zehnder (MZ) or Sagnac interferometric receiver without requirement of any external phase reference.**

***Index Terms*— Acoustooptic deflector, coherent modulation/demodulation, differential phase shift keying (DPSK), electrooptic demodulation, femtosecond mode locked laser, optical fiber communication, optical fiber dispersion, optical frequency conversion.**

I. Introduction

RECENT developments of spectral phase and amplitude modulation techniques permit shaping of femtosecond (fs) laser pulses, which is an attractive technology for terabit per second (Tb/s) communication systems. Several research groups have explored pulse shaping applications such as generating arbitrary fs pulse sequences for optical time division multiplexing (OTDM) transmission [1]–[3], optical signals for spread time code division multiple access (CDMA) [1], [4], [5], or spectrally modulated fs pulses for wavelength division multiplexing (WDM) transmission [3], [6], [7].

Phase modulation is often superior to amplitude modulation for communication applications, since an amplitude modulator will generally throw away 50% of the transmitter power. Unfortunately, optical direct detection devices as normally used are sensitive only to the amplitude of the laser pulses. In a spectral modulation system employing a fs pulse shaper, each spectral element has a well defined phase relation with respect to all others, since all spectral elements are derived from a single fs pulse. We utilize this coherence property embedded in the optical frequency domain to propose a novel coherent optical communication scheme, which we term *frequency-domain differential phase shift keying* (FD-DPSK). We also present appropriate receiver designs for such a spectrally modulated fs-pulse OTDM optical communication network, using a Mach–Zehnder or a Sagnac interferometer. Both Mach–Zehnder and Sagnac FD-DPSK receivers are capable of handling OTDM channel drop and demodulation of FD-DPSK simultaneously. We demonstrate the feasibility of these receivers by computer simulations. Finally, we show a Mach–Zehnder FD-DPSK receiver can achieve higher performance in a noisy network than a direct detection receiver for a comparable ASK signal.

Manuscript received October 2, 1996; revised July 3, 1997. This work was supported by the DOD/BMDO and AFOSR under the Photonics for Data Fusion program through Princeton University.

J.-K. Rhee is with NEC Research Institute, Princeton, NJ 08540 USA.

H. Kobayashi is with the Advanced Technology Center for Photonics and Optoelectronic Materials and Department of Electrical Engineering, Princeton University, Princeton, NJ 08544 USA.

W. S. Warren is with the Advanced Technology Center for Photonics and Optoelectronic Materials and Department of Chemistry, Princeton University, Princeton, NJ 08544 USA.

Publisher Item Identifier S 0733-8724(97)08891-9.

II. Background

Recently, Hillegas *et al.* demonstrated programmable femtosecond optical pulse shaping using a spatial acoustooptic modulator (AOM) in a zero-dispersion line [8]. Although the principle of pulse shaping is the same as other technologies, an AOM pulse shaper potentially has advantages for practical applications in optical communications because of its fast update rate and availability at lower costs. Other technologies employing a liquid crystal modulator (LCM) array [1], [2] and a semiconductor electrooptic modulator array consisting of GaAs/AlGaAs quantum well devices [6] are demonstrated, but LCM arrays have slow update rates (≈milliseconds), and semiconductor modulator arrays with high spatial resolution are not yet commercially available.

A typical AOM pulse shaper has 100 to 1000 bit effective spectral modulation resolutions with 1–10 μs access times, and allows data coding speeds from 0.1 to 1 Gb/s, depending on the aperture size and the modulation bandwidth of the AOM. Thus, an fs laser and AOM pulse shaper in an optical communication system as the transmitter can achieve a subscriber-to-subscriber transmission from 0.1 to 1 Gb/s. However, such a system would achieve this transmission rate with an extremely low duty cycle, permitting aggregate throughputs higher than a Tb/s with multiplexing [9].

Fig. 1 shows an example architecture of a Tb/s OTDM spectral-modulation communication network that uses the AOM pulse shaper technology, as suggested by Warren and his collaborators [3], [7]. Each transmitter consists of a synchronized 100-fs pulse laser and an AOM pulse shaper. The gratings, lens, and AOM sequence of G1, L1, AOM, L2, and G2 forms a pulse shaper [3], [8]. In this example, the aperture

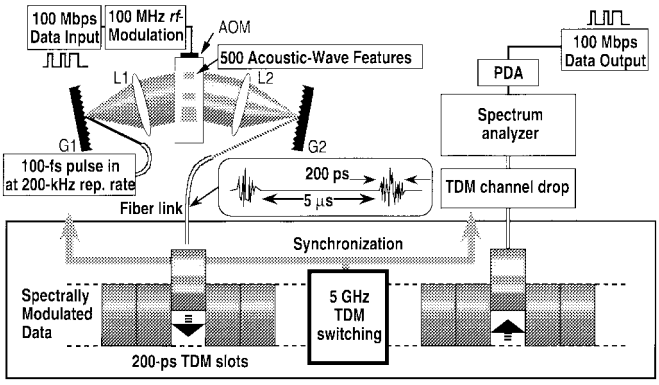

Fig. 1. Proposed architecture of a Tb/s, femtosecond-pulse WDM system using a high-resolution spatial acoustooptic modulator. A transmitter includes a 100-fs modelocked laser and a high resolution acoustooptic pulse shaper. In the pulse shaper, a spectrum of a 100-fs optical pulse is modulated in phase and amplitude by 500-bit data using a 100-MHz bandwidth, traveling-wave acoustooptic modulator (AOM) in a zero-dispersion line consisting of gratings (G1, G2) and lenses (L1, L2). (See [3], [8], and [9] for experimental demonstrations.) The modulated signal occupying only a 200-ps time window, is then multiplexed in a 5-GHz OTDM system and demultiplexed at a receiver. The resulting signal can be analyzed by a spectrometer for detection of a signal in each spectral element. PDA stands for a photodetector array.

size of the AOM is 20 mm, which corresponds to an access time of $\approx$5 μs, and the carrier frequency and the modulation bandwidth are 200 MHz and 100 MHz, respectively. The input data sequence at 100 Mb/s is converted to a radio-frequency (RF) signal with a 100-MHz modulation bandwidth. The RF signal then creates a traveling acoustic wave in the AOM. An acoustic waveform containing 500-bits of information completely fills the aperture of the modulator in 5 μs. At this point, the spectrum of a 100-fs pulse, generated by the gratings and lens, is sent through the modulator and deflected with the amplitude and phase information of the modulating RF waveform. As a result, the full bandwidth of 5 THz of a 100-fs pulse is sliced into spectral elements with 10-GHz bandwidth. Since the spectral profile is approximately rectangular, each spectral element occupies a 200-ps time window by the Fourier transform relation. The output pulse is a superposition of all modulated spectral elements and occupies the same 200-ps time window every 5 μs. Thus, incorporating 25 000 transmitters in a 5-GHz OTDM network, we can achieve, in principle, 2.5-Tb/s aggregate throughput, in an ideal system, or a short haul fiber communication system.

An important feature of this scheme is that users can select an arbitrary transmission speed up to the modulation bandwidth of the AOM, without requirement of any adjustment of the OTDM switching system. This transmission scheme is useful for a local area network with a large number of users for access to highly fused data transmission. In practice, there will be a limit set by interference or crosstalk between high-density spectrum-sliced elements. Note here that one 100-fs pulse with 5-THz bandwidth is sliced into 10-GHz spectral elements containing 500 bits of information, and that each spectral element is phase coherent with all other elements, for a moderate distance of optical fiber transmissions up to a few kilometers.

III. Schematic of Optical FD-DPSK

In FD-DPSK, a transmitted data sequence is coded as the phase difference between a pair of adjacent spectral elements of the shaped optical signal, as opposed to the conventional (time domain) differential shift keying method. At the receiver side, we wavelength-shift a received optical signal by the separation of the spectral elements, and interfere wavelength-shifted and unshifted signals to produce an amplitude modulated optical signal for detection. This FD-DPSK scheme eliminates the requirement for either a phase reference pulse from the transmitter or a local oscillator as required in a traditional coherent optical communication system. Note that performance of conventional heterodyne detection with a local oscillator is limited because the detection is extremely sensitive to phase error in the signal or the local oscillator [10], [11].

In the conventional DPSK the carrier is modulated with phase symbols corresponding to a differential symbol sequence in the time domain and the received signal is demodulated by detecting phase rotation between successive symbol phases. As an example of binary DPSK, we consider an n-bit binary sequence $a_i \in \{0,1\}$. The corresponding DPSK sequence $\{b_0, \cdots, b_n\}$ is defined by the following relation:

$$b_i = \begin{cases} 0, & \text{for } i = 0, \\ (a_i + b_{i-1}) \bmod 2, & \text{for } i = 1, 2, \cdots n, \end{cases} \tag{1}$$

where "mod 2" stands for modulo 2 arithmetic. The phase symbols are then given by

$$\phi_i = \pi b_i. \tag{2}$$

An n-bit DPSK sequence requires $(n+1)$ bit transmission, since we retrieve transmitted data by phase differences between successive bits. In an ordinary RF communication system, DPSK is implemented as a sequence in the time domain. The differential phase between successive bits is obtained by either interfering or mixing the received input signal and its replica with a delay of the time interval occupied by one bit information.

However, in the FD-DPSK approach, the differential phase is introduced as the phase difference between adjacent spectral elements of a coherent spectral-modulation system; the information is retrieved by an interferogram between adjacent spectral elements by means of a wavelength shift. First consider a transform-limited ultrashort optical pulse in the frequency domain. (Here, we denote optical frequency abbreviately as frequency.) We assume that the portion of the pulse spectrum that will be used for communication has a constant amplitude profile with spectral bandwidth $\Delta\omega$, but it is straightforward to generalize the analysis. The spectrum is then sliced into $(n+1)$ spectral elements for spectral modulation

$$\tilde{E}_c(\omega) = \sum_{i=0}^{n} C \ \text{rect}(\omega - \omega_i, \delta\omega) \tag{3}$$

where $\tilde{E}_c(\omega)$ is the (complex) field amplitude as a function of optical frequency ω, C is a constant, and the rectangle function

is defined as

$$\text{rect}(x,a)=\begin{cases}1, & \text{for } -|a|/2\le x\le |a|/2,\\ 0, & \text{otherwise.}\end{cases} \tag{4}$$

For the sake of convenience, we assume $C=1$ hereafter. The central frequency and the bandwidth of the ith element are given by $\omega_i=\omega_0+i\delta\omega$ and $\delta\omega=\Delta\omega/(n+1)$, respectively, where ω_0 is the central frequency of the spectral element at the longest wavelength. The differential shift keying sequence can be phase-modulated in the coherent optical pulse using the conventional DPSK definition in (1) and (2), except now the phase differences are between spectral elements, by use of the aforementioned pulse shaping transmitter. We express the phase-modulated spectral signal as

$$\tilde{E}_s(\omega)=\sum_{i=0}^{n}\exp(j\phi_i)\ \text{rect}(\omega-\omega_i,\delta\omega). \tag{5}$$

A simple FD-DPSK receiver consists of either a Mach–Zehnder or Sagnac interferometer with a device for a wavelength shift corresponding to an optical frequency shift by $+\delta\omega$ on one arm, and an n-channel spectrum analyzer with $\delta\omega$ resolution as the detector. Fig. 2 shows an example of a simple Mach–Zehnder FD-DPSK receiver. The signal traveling on the lower arm of the Mach–Zehnder interferometer experiences a wavelength shift. The wavelength-shifted $(i-1)$th element will then have the same central frequency as that of the unshifted ith element

$$\exp(j\phi_{i-1}+j\Delta)\ \text{rect}(\omega-\omega_i,\delta\omega).$$

Here Δ is the phase difference in the transmission direction between the two arms of the interferometer; for simplicity of analysis, we set $\Delta=0$. Then, the ith element on the detector can be obtained by (6a)–(6c) shown at the bottom of the page. Here, factor $1/2$ is introduced because of the configuration of a Mach–Zehnder interferometer. Using the relation $a_i=(b_i-b_{i-1})$ mod 2 derived from (1), we find the corresponding power spectrum for $i=1,2,\cdots n$:

$$\begin{aligned}I^i_{\text{det}}(\omega)&=\left|\tilde{E}^i_{\text{det}}(\omega)\right|^2\\&=\frac{1}{2}\text{rect}(\omega-\omega_i,\delta\omega)[1+\cos(\pi a_i)].\end{aligned} \tag{7}$$

Thus, the phase information is converted to the intensity modulation which corresponded to the input data sequence of the transmitter. Note that a bit of zero $(a_i=0)$ produces the intensity of one unit on the detector.

Although we limit the description to a binary system, this FD-DPSK scheme can be extended to an m-ary system. In an m-ary system, the differential phase encoding (2) should take the form

$$\phi_i=\begin{cases}0, & \text{for } i=0,\\ \psi(a_i)+\phi_{i-1}, & \text{for } i=1,2,\cdots n\end{cases} \tag{8}$$

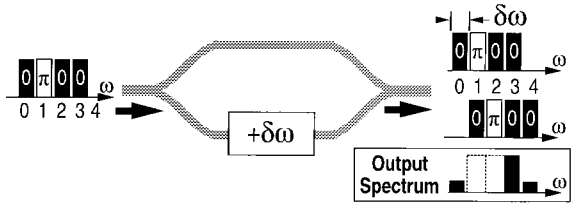

Fig. 2. Schematic of a simple FD-DPSK receiver. The receiver is realized with a Mach–Zehnder interferometer and a coherent wavelength (frequency) shifter denoted as $+\delta\omega$. The input signal is split and combined after a wavelength shift on one arm of the interferometer. The spectra at the combiner and the output interference spectrum of the two signals are indicated on the right-hand side.

where $\psi(a_i)$ is a phase function with which we can uniquely decode the symbol $a_i\in\{0,1,\cdots m-1\}$. Then the generalized form of the detection (7) for an m-ary system is given by

$$I^i_{\text{det}}(\omega)=\frac{1}{2}\text{rect}(\omega-\omega_i,\delta\omega)[1+\cos(\psi(a_i))]. \tag{9}$$

In a simple phase detection achieved by (9), an assignment of $\psi(a_i)$ over 2π range will cause redundancy. The phase redundancy may, of course, be eliminated by detection in another quadrature with a $\pi/2$ phase difference between the two arms of the interferometer. In order to keep the detection system simple, however, we consider phase variations only in the range from 0 to π. In a low-noise system, $\psi(a_i)$ can be assigned in any arbitrary manner. However, in a practical system in the strong-noise limit, we can reduce detection errors by having the value assignment of $1+\cos(\psi(a_i))$ equally spaced in the intensity domain, by the following relation:

$$\psi(a_i)=\cos^{-1}(1-2a_i/(m-1)). \tag{10}$$

Although there is no theoretical upper limit for the integer m, we explicitly demonstrate the feasibility of an FD-DPSK system for $m=2$ (the binary DPSK case, $\psi(a_i)=\pi a_i$) as implemented in (1), (2), and (7). In the next section, we propose receiver designs for practical applications, employing normally-off interferometers.

IV. Practical FD-DPSK Receiver Designs

Generating a wavelength shift of one spectral element spacing is the most challenging feature of an FD-DPSK receiver. Wavelength shifts can be achieved by electrooptic phase modulators (EOPM), AOM's, four-wave mixing devices, and saturable-gain semiconductor optical amplifiers [12]. However, the wavelength shift must retain phase information in the output, and must be comparable to the optical resolution limit. Such a shift is relatively large (corresponding to an optical frequency shift of ≈10 GHz) for a modulator system. Considering coherence and efficiency, an EOPM synchronized to an input pulse train is a good choice for the wavelength

$$\tilde{E}^i_{\text{det}}(\omega)=\begin{cases}\frac{1}{2}\text{rect}(\omega-\omega_0,\delta\omega)\exp(j\phi_0), & \text{for } i=0 \quad (6a)\\ \frac{1}{2}\ \text{rect}(\omega-\omega_i,\delta\omega)[\exp(j\phi_{i-1})+\exp(j\phi_i)], & \text{for } i=1,\ldots,n \quad (6b)\\ \frac{1}{2}\text{rect}(\omega-\omega_{n+1},\delta\omega)\exp(j\phi_n), & \text{for } i=n+1 \quad (6c)\end{cases}$$

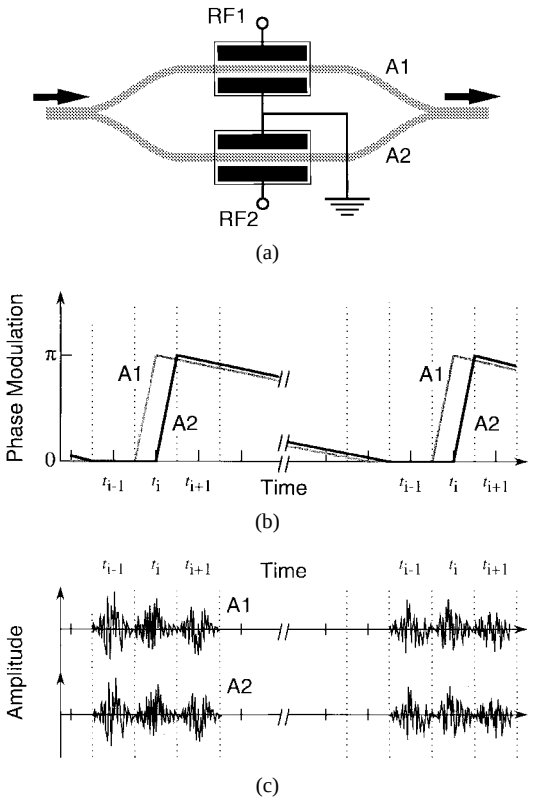

Fig. 3. FD-DPSK Mach–Zehnder receiver; (a) schematic of the receiver; (b) the phase modulation in the electrooptic phase modulators; and (c) an illustration for the demodulation principle. The receiver consists of a pair of fast electrooptic phase modulators and a Mach–Zehnder interferometer. Radio-frequency voltages (RF1 and RF2) are applied to produce phase modulation on each arm as shown in (b). Shaded regions in (c) indicate the corresponding wavelength-shift windows for light traveling in arms A1 and A2 of the interferometer.

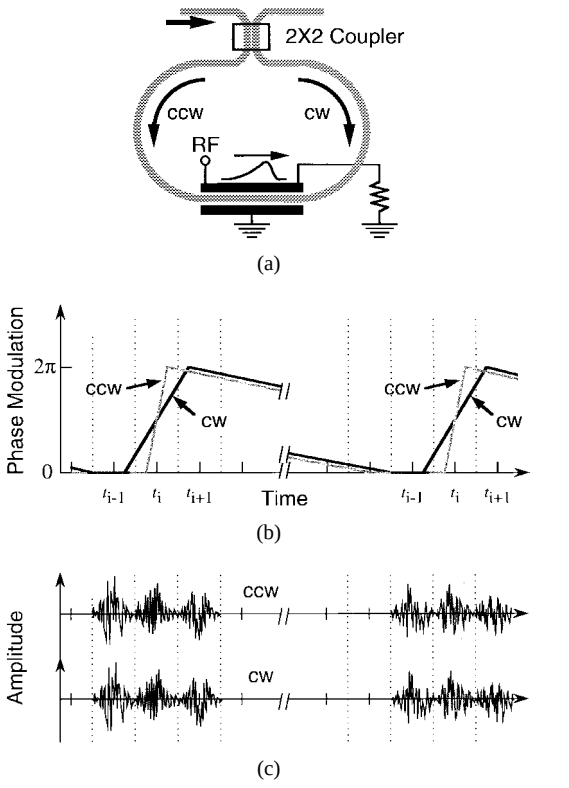

Fig. 4. FD-DPSK Sagnac receiver; (a) schematic of the receiver; (b) the phase modulation in the electrooptic phase modulator; and (c) an illustration of the demodulation principle. The receiver consists of a fast traveling-wave electrooptic modulator and a fiber Sagnac loop. Radio-frequency voltage (RF) is applied to produce phase modulation on each traveling direction as shown in (b). Shaded regions in (c) indicate the corresponding wavelength-shift windows for the light signals in each direction. ccw and cw stand for counter clock-wise and clock-wise, respectively.

shift. In the configuration shown in Fig. 2, an EOPM for the wavelength shift is implemented in the lower arm. A ramp bias to the modulator produces a wavelength shift. The amount of wavelength shift corresponds to an optical frequency shift given by the slope of the phase variation in the time domain. Therefore, we can demodulate an FD-DPSK signal in the way described in the previous section.

In order to maximize throughput, it is desired to multiplex FD-DPSK signals from multiple transmitters into an OTDM system, because the FD-DPSK signal is an optical wave packet occupying only a $\approx 2\pi/\delta\omega$ temporal range. In this case, a receiver with a time gated wavelength shift ought to be capable of handling OTDM demultiplexing and FD-DPSK demodulation. We can realize such receivers using a Mach–Zehnder or Sagnac interferometer (Figs. 3 and 4).

A Mach–Zehnder receiver consists of a normally-off optical Mach–Zehnder interferometer and a pair of EOPM's on both arms [Fig. 3(a)]. Because we require a modulation bandwidth greater than 10 GHz, the receiver ought to be integrated into a wave-guide structure. An input FD-DPSK signal is split into two arms A1 and A2. Then we apply identical ramp RF biases to the modulators, but with a time delay corresponding to nearly one half of the OTDM slot. Since the phase is, to the first order, proportional to the bias, we can introduce a linear phase variation by the bias ramp, which has a slope corresponding to the spectral element spacing $\delta\omega$. As shown in Fig. 3(b), suppose that the phase modulation of arm A1 leads that of A2. Then the first half part of the light signal traveling in arm A1 is wavelength shifted and the corresponding part of arm A2 is not; in the second half, the light in arm A2 is wavelength shifted and the corresponding part of arm A1 is not [Fig. 3(c)]. As a result, we produce the desired interference of the two light signals at the output side of the Mach–Zehnder interferometer. Analyzing the spectrum of the output with, for example, a spectrometer and a photodiode array, we obtain the spectral intensity modulation of (7). Subsequently, we decrease the demodulation bias with a sufficiently large time constant, keeping the phase modulations of the two arms nearly the same. Thus, the output light is turned off during this relaxation period in the normally-off Mach–Zehnder interferometer; the wavelength shift and interference take place only during a given OTDM time slot. Therefore, we achieve simultaneous OTDM demultiplexing and FD-DPSK demodulation.

In a similar way, we can realize an FD-DPSK receiver in a Sagnac fiber loop with a traveling-wave EOPM. The design of the Sagnac receiver is shown in Fig. 4(a). A Sagnac fiber loop is normally a mirror because of destructive interference in the transmission port between clockwise (cw) and counter-clockwise (ccw) traveling light. When light travels in both directions it experiences exactly the same phase variation in

the fiber loop. However, a fast RF bias to the traveling-wave EOPM introduces different phase modulations for different directions, as shown in Fig. 4(b); the ccw light which co-propagates with the RF bias experiences fast modulation whereas the cw light (counter-propagating direction) experiences slow modulation. If a ramp bias is applied, the light signals in both directions are wavelength shifted, but by different amounts. The height of the shading in Fig. 4(c) indicates the degree of wavelength shift. When the difference of the wavelength shifts between in the two directions corresponds to $\delta\omega$, the FD-DPSK is converted into an amplitude modulation on the transmission port of the Sagnac loop. In order for simultaneous OTDM demultiplexing and FD-DPSK demodulation, we apply the ramp bias only during a selected OTDM slot and decrease it with a sufficiently large time constant. Therefore, we block signals in other OTDM slots from transmission. However, because of the slow modulation on the counter-propagating light signal, this receiver design involves a problem of signal leakage from adjacent OTDM slots. (In Fig. 4(b), the phase modulation of cw signal expands outside the selected OTDM slot.)

Both Mach–Zehnder and Sagnac receivers require precise synchronization of the RF bias to excite the EOPM at the correct time. This can be achieved with a current technologies of optical clock recovery and picosecond electronic pulse generation. Clock recovery in the present OTDM system can be achieved by sampling one spectral element with a narrow band wavelength coupler. In general, a typical all-optical clock recovery system reproduces clock signals with timing jitter on the order of 1 ps in a Gb/s OTDM system [13]–[15], Although typical jitter of high precision RF electronics is on the order of 10 ps, this jitter is not a problem of FD-DPSK demodulation as discussed in the following section.

V. Analysis

We have modeled the proposed FD-DPSK receivers to evaluate the feasibility and performance with computer simulations, in order to investigate the characteristics of the receivers associated with operational parameters such as the slope and the maximum voltage of the demodulation RF ramp bias; to test how robust the FD-DPSK scheme is against noise, compared with a direct-detection amplitude shift keying (ASK) scheme; and to investigate problems associated with timing jitter in a receiver and fiber dispersion.

A. Mach–Zehnder FD-DPSK Receiver

The most interesting feature of a Mach–Zehnder receiver is to apply the ramp biases with different time delays so as to time gate wavelength shift only during a selected OTDM slot. Thus, it is simpler to model the characteristics in the time domain. Consider a time-domain input light signal modulated with FD-DPSK. The time-domain input signal $E_m(t)$ is obtained by the inverse Fourier transform of $\tilde{E}_m(\omega)$. In a normally-off Mach–Zehnder interferometer, the signals at the output port that have traveled through arms A1 and A2 are given as $+\frac{1}{2}E_m(t)$ and $-\frac{1}{2}E_m(t)$, respectively. By applying RF biases to the EOPM's as depicted in Fig. 3(b), we obtain the output signal of the Mach–Zehnder interferometer as follows:

$$E_{\mathrm{dem}}(t) = \frac{1}{2}[E_m(t)\exp(j\delta\omega T_r\mu(t+T_r/2)) - E_m(t)\exp(j\delta\omega T_r\mu(t-T_r/2))] \quad (11)$$

and the profile of the RF bias applied to the EOPM's for demodulation of FD-DPSK is given by

$$\mu(t) = \left(\frac{1}{2}+\frac{t}{T_r}\right)\mathrm{rect}(t,T_r) + \left(\frac{1}{2}-\frac{t-t_f}{T_f}\right)\mathrm{rect}(t-t_f,T_f). \quad (12)$$

Here, T_r and T_f are the rise and fall times of the triangle-shape function $\mu(t)$ with a sharp rise edge and a slow fall tail ($T_r \ll T_f$), and $t_f = (T_r+T_f)/2$. In the rise edge, the wavelength shift due to the phase sweep, i.e., due to the linear phase variation corresponds to $\delta\omega$, or the spectral element spacing. This element spacing (and the maximum phase excursion in the modulator) determines the optimal value of T_r. The choice of different T_f has little effect on the receiver operation and $T_f = 1$ ns is used. Fourier transforming the demodulated time-domain signal $E_{\mathrm{dem}}(t)$, we finally obtain the power spectrum corresponding to the original data sequence $\{a_i\}$.

We have simulated our model for a seven-bit case ($n = 7$) to find an optimal choice of T_r and to study noise characteristics of the FD-DPSK system. We assume $\delta\omega/2\pi = 10$ GHz, which corresponds to a 0.08-nm spectral resolution at 1.55 μm. Fig. 5(a) shows a typical example of an FD-DPSK spectral amplitude signal ($\{b_0,\cdots,b_7\} = \{1,0,1,0,0,0,1,1\}$), Fig. 5(b) the corresponding spread time amplitude signal, and Fig. 5(c) the power spectrum demodulated at the receiver. Here DPSK symbols b_0 to b_7 are assigned to spectral elements equally spaced in the optical frequency detuning range from -40 to 40 GHz. (e.g., b_0 occupies the frequency detuning range from -40 to -30 GHz.) Accordingly, we find the demodulated symbols $\{a_1,\cdots,a_7\} = \{0,0,0,1,1,0,1\}$ as the inverse of the intensities in the frequency detuning range from -30 to 40 GHz in Fig. 5(c), which agrees with (7). We find $T_r = 55$ ps for the maximal discrimination between "0" and "1." It is interesting that although the Mach–Zehnder receiver is normally off so that the result of (7) has to be inverted, the result is the same as that for a normally-on interferometer. It is because near $t = 0$ we have constructive interference for arms A1 and A2. In Fig. 5(d), we present a simulated eye diagram *in the frequency domain* for the noise-free case to show the detectability of the receiver. The eye diagram is generated by plotting the power spectra of the receiver for all possible 2^7 cases of $\{a_i\}$ sequence. We clearly see open eyes for all spectral elements.

B. Sagnac FD-DPSK Receiver

In modeling the Sagnac receiver, we first consider the rise times of the phase modulation in co- and counter-propagating directions in a traveling-wave EOPM. The instantaneous refractive index modulation is proportional to an integral of

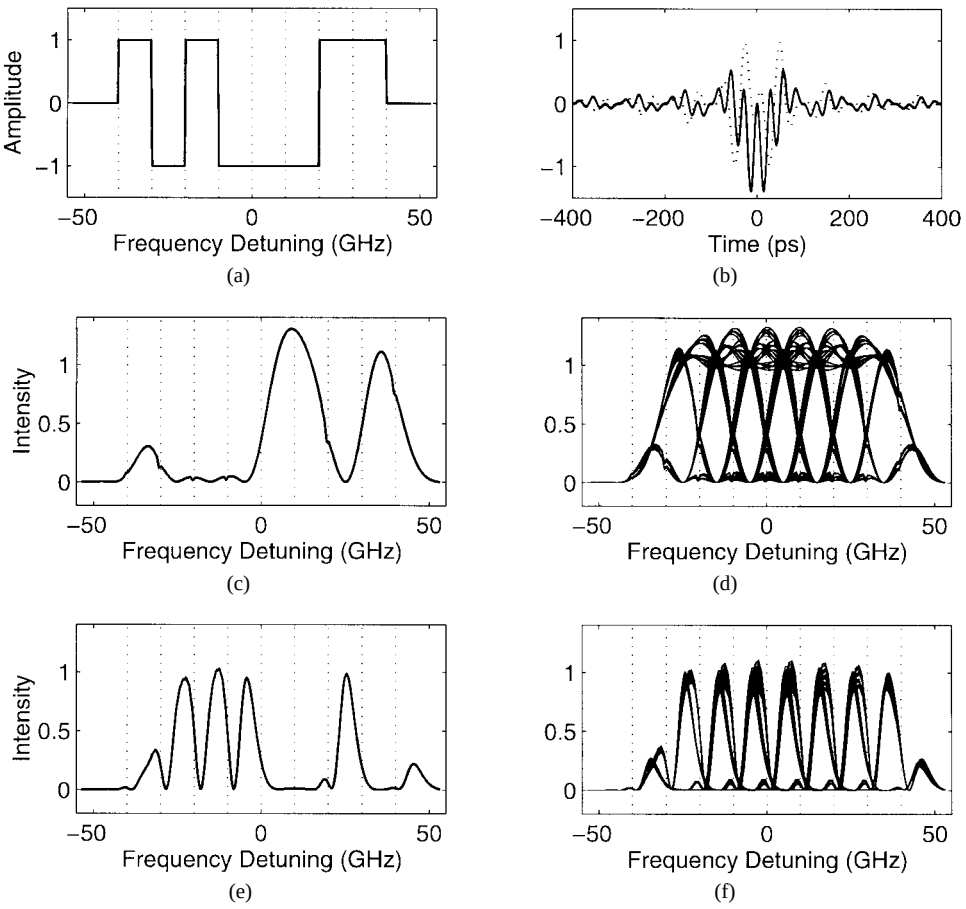

Fig. 5. Simulation results of the FD-DPSK receivers. In (a) and (b), we show, respectively, a typical example of FD-DPSK signal in the optical frequency domain and the corresponding temporal waveform (solid curve for real part and dotted curve for imaginary part) for $n = 7$ case. The differential data sequence $\{b_0, \cdots, b_7\}$ is assigned to the eight frequency bins from -40 to 40 GHz. In (c) and (e), we show output spectra of, respectively, a Mach–Zehnder receiver and a Sagnac receiver corresponding to the input signal shown in (a). The demodulated data sequences $\{a_1, \cdots, a_7\}$ for each case are found in the frequency bins from -30 to 40 GHz. We also show calculated noise-free eye diagrams in the frequency domain in (d) and (f), respectively for the Mach–Zehnder and Sagnac receivers. The vertical units are arbitrarily chosen.

interaction between the instantaneous RF electric field and the traveling frame of light within the traveling-wave electrode. The phase modulation is expressed as

$$\Delta\phi = k_0 \int_{-\frac{L}{2}}^{+\frac{L}{2}} \int_{-\infty}^{+\infty} \Delta n_{\max} \mu(t' - x'/c) \times \delta(t' - t \mp x'/c)\, dt'/dx' \tag{13}$$

where L is the length of the traveling-wave electrode in the EOPM, $\Delta n_{\max}$ is the index modulation depth, $\mu(t)$ is defined in (12), k_0 is the magnitude of the wave vector in the free space, and c is the speed of light in the wave guide which is matched to the speed of the traveling RF field. Here Dirac delta function $\delta(t' - t \mp x'/c)$ defines the time t' and position x' of the light signal with a relative delay of t, which is modulated by the RF electric field. The "$-$" and "$+$" signs indicate, respectively, the co- and counterpropagation directions. For a copropagating light signal, (13) becomes

$$\Delta\phi_{\rm co}(t) = k_0 L \Delta n_{\max} \mu(t). \tag{14}$$

Here, we define $\delta\omega_{\rm Sag}$ as in $\delta\omega_{\rm Sag} T_R = k_0 L \Delta n_{\max}$, i.e., the slope of phase variation in the rise edge. For the light field in the counterpropagation direction, (13) can be written as

$$\Delta\phi_{\rm cntr}(t) = k_0 \int_{-\frac{L}{2}}^{+\frac{L}{2}} \Delta n_{\max} \mu(t - 2x'/c)\, dx' \tag{15}$$

$$= \frac{1}{2} k_0 \Delta n_{\max} \int_{-\infty}^{+\infty} \text{rect}(x, 2L) \mu(t - x/c)\, dx. \tag{16}$$

The modulation speed of the counter-propagating light field decreases with L. When $T_R < L/c$. The rise time of $\phi_{\rm cntr}(t)$ is $\approx 2L/c$, twice the transit time of the traveling wave modulator. Thus, the frequency shift near $t = 0$ is $ck_0\Delta n_{\max}/2$, or $\delta\omega_{\rm Sag} T_R c/2L$. In order to achieve interference between each pair of adjacent spectral elements, the $(i-1)$th element in the copropagation direction ought to have the same central frequency as that of ith element in the counterpropagation direction. Therefore, we should select $\delta\omega_{\rm Sag} = (1 - T_R c/2L)^{-1} \delta\omega$. Note that the center of the modulator wave guide should coincide with the center of the Sagnac loop in order to have the same modulation timing for light signals in both co- and counterpropagation directions.

The signals traveling in the ccw and cw directions at the transmission port (Fig. 4) are $+\frac{1}{2}E_m(t)$ and $-\frac{1}{2}E_m(t)$

respectively, because a Sagnac loop is normally-off. Finally, we find the demodulated signal

$$E_{\rm dem}(t) = \frac{1}{2}[E_m(t)\exp(j\phi_{\rm co}(t)) - E_m(t)\exp(j\phi_{\rm cntr}(t))]. \tag{17}$$

The power spectrum for the original data sequence $\{a_i\}$ can be obtained by Fourier transforming the demodulated time-domain signal $E_{\rm dem}(t)$.

We have also computer simulated the output spectrum from the Sagnac receiver for the same input data as for the Mach–Zehnder receiver. We assume that the traveling wave EOPM consists of a lithium niobate ($LiNbO_3$) waveguide and an electrode with a length L of 2 cm. The results given in Fig. 5(e) and (f) show the demodulated receiver output power spectrum for the given data sequence $\{a_1, \cdots, a_7\} = \{0,0,0,1,1,0,1\}$ and the eye diagram in the frequency domain for a noise-free case, respectively. In contrast to the Mach–Zehnder case, the demodulated signal is not inverted, because the output signal near $t = 0$ has a destructive interference in the output port. We used $T_r = 100$ ps, $T_f = 1$ ns, and $\delta\omega_{\rm Sag}/2\pi = 12$ GHz, for the maximal discrimination between "0" and "1." The results clearly demonstrate that a Sagnac receiver detects FD-DPSK signals.

C. Noise Characteristics of FD-DPSK Receivers

Phase shift keying and coherent detection generally achieve lower bit error rates compared with that of an ASK and direct detection method, although this is not always true for optical communication systems due to the laser phase noise in transmitters and receivers [16]. We can achieve higher performance with FD-DPSK than with an ASK and direct detection method in a noisy communication system. In this section, we simulate and compare the noise characteristics for FD-DPSK and ASK.

We tested the receivers with signals in a harsh network condition, i.e., a signal-to-noise ratio (SNR) of 1, so as to clearly demonstrate the comparisons of detectability among ASK with direct detection, FD-DPSK with a Mach–Zehnder receiver, and FD-DPSK with Sagnac receiver. We assume both ASK and FD-DPSK signals are generated from an ideal femtosecond laser source with the same amplitude, and both cases employ an identical OTDM network.

In order to model noises in both phase and amplitude we added white noise to the time-domain input signal. The white noise is generated from a random number sequence with Gaussian distribution. To obtain noisy signals with an SNR of 1, the standard deviation of the noise is adjusted to be the same as the amplitude of the input signal. Under this low SNR condition, the signal is hardly visible in the time domain. However, the signal in the frequency domain after OTDM demultiplexing is detectable in both ASK and FD-DPSK cases.

Fig. 6 shows calculated eye diagrams in the frequency domain for (a) FD-DPSK with a Mach–Zehnder receiver, (b) FD-DPSK with a Sagnac receiver, and (c) ASK and direct detection. The input data sequences are generated randomly, and the white noise is added to the signals in the time domain. We use the same system parameters as in the previous sections for FD-DPSK receivers. The ASK receiver output signal is obtained after OTDM demultiplexing, i.e., we time gate the noisy ASK signals with the same temporal window size as for FD-DPSK, namely 100 ps. Interestingly enough, the eye diagrams show a clear enhancement of detectability against the noise only with the FD-DPSK Mach–Zehnder receiver. The eye pattern from the Sagnac receiver is worse than the ASK and direct detection. It is because the Sagnac receiver is not a robust OTDM demultiplexer due to the slow phase modulation in the counter-propagating light during a time window wider than a OTDM slot.

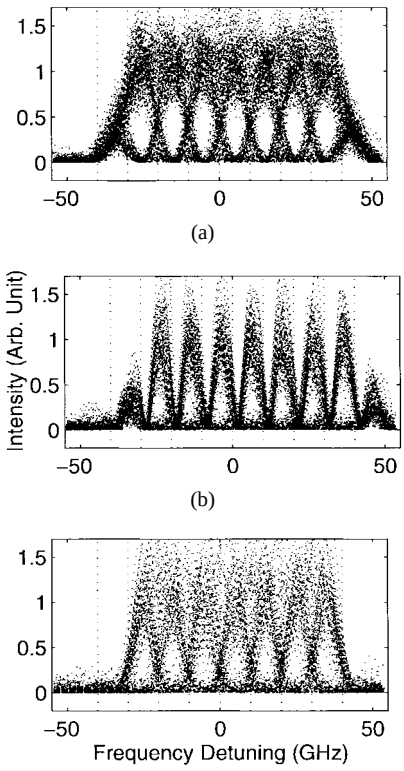

Fig. 6. Simulated eye diagrams for (a) FD-DPSK demodulated by the Mach–Zehnder receiver, (b) FD-DPSK by the Sagnac receiver, and (c) a comparable ASK with direct detection. The SNR is assumed to be "1." The eye diagrams are generated with multiples of random data sequences and with amplitude and phase noise generated from random numbers with Gaussian distribution.

D. Timing Jitter and Fiber Dispersion

When the FD-DPSK scheme is implemented with the proposed receivers, fundamental difficulties associated with clock jitter and fiber dispersion may arise. We can understand both jitter and dispersion as a unified problem with phase variation in the frequency domain, since an arbitrary delay due to clock jitter and fiber dispersion correspond respectively to the first-order and the second- or higher order phase variations in the frequency domain. In the following analysis, we show that both problems will not necessarily prevent a practical implementation.

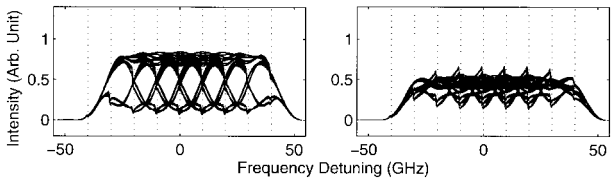

Fig. 7. Simulated eye diagrams of the FD-DPSK scheme with receiver clock timing errors of (a) 20 ps and (b) 30 ps. A Mach–Zehnder receiver is assumed.

The FD-DPSK signal with jitter and dispersion is modeled by including a phase factor in (5)

$$\tilde{E}_s(\omega) = \sum_{i=0}^{n} \exp(j\phi_i)\ \mathrm{rect}(\omega - \omega_i, \delta\omega) \times \exp(-j\tau\omega - j\beta(\omega)L) \tag{18}$$

where τ is the time delay, L is the length of the fiber link, and $\beta(\omega)$ is the dispersion given by

$$\beta(\omega) = \frac{1}{2}b_2(\omega - \omega_c)^2 + \frac{1}{6}b_3(\omega - \omega_c)^3. \tag{19}$$

Here, $b_2 = -D\lambda_c/\omega_c, b_3 = 3S_0\lambda_c^2/\omega_c^2$, where λ_c and ω_c are, respectively, the wavelength and frequency of the spectral element at the center of transmitted spectral data, and D and S_0 are the fiber dispersion and the dispersion slope, respectively. The effect of parameter S_0 is negligible in normal fiber, but becomes dominant in dispersion shifted (DS) fiber where dispersion is given by $D = S_0(\lambda - \lambda_0)$ and is nearly zero. (Here, λ_0 is the wavelength where the dispersion becomes zero.) Now we can apply demodulation to the signal given by (18), by use of either the Mach–Zehnder or the Sagnac receiver as described in the previous sections, in order to investigate the effect of jitter and dispersion. Here, we present the result of the Mach–Zehnder receiver case.

First, we study the jitter problem by setting $b_2 = 0$ and $b_3 = 0$, and introducing a nonzero time delay equivalent to a possible clock jitter in a receiver. Fig. 7(a) and (b) presents calculated eye diagrams for $\tau = 20$ and 30 ps, respectively. As shown, we can see a clear opening of an eye diagram even at a time delay of 20 ps. However, there is serious deterioration of the eye pattern for delays longer than 30 ps, because the adjacent spectral elements have relative phase evolution in time given by the frequency separation of 10 GHz. The relative phase between adjacent spectral elements have 2π phase rotation during the 100-ps signal pulse width. Setting a strict criterion for phase error of FD-DPSK signal, we can tolerate phase error less than $\pi/2$, or equivalently 25-ps timing error, which is achievable with the state-of-the-art technologies for optical clock recovery [13]–[15] and picosecond electronics.

Second, the problem of dispersion shows more significant effect because different spectral elements arrive at different times. Interestingly, the deterioration of signal is associated with group delay dispersion $\frac{d\beta}{d\omega}$ rather than with phase error $\beta(\omega)$ between adjacent spectral elements. Fig. 8(a) shows computer simulation result of an eye diagram of a Mach–Zehnder receiver output, when the signal is received from a 6-km-long normal fiber link. Here we used $D = 16$ ps/nm · km for a 1.55-μm application and set $\tau = 0$ and $b_3 = 0$. The signal in the middle of the wavelength range show white spaces for discrimination between "0" and "1." However, the spectral elements on the sides show a problem in detection.

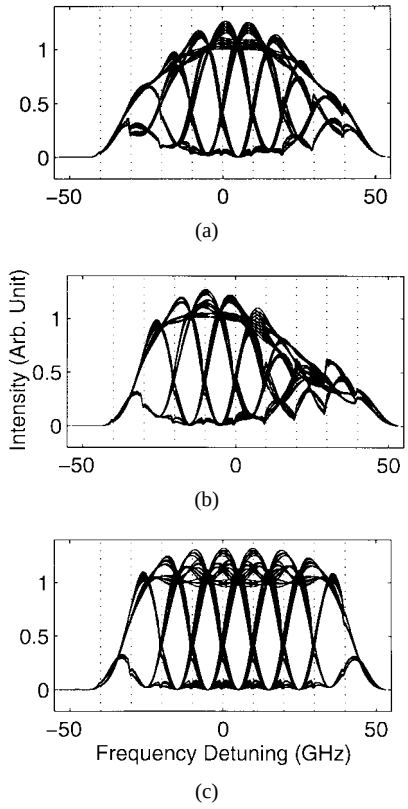

Fig. 8. Simulated eye diagrams of the FD-DPSK scheme with fiber dispersion effects from, (a) a 6-km normal fiber link, (b) the same link with an added 10-ps delay, and (c) a 1000-km dispersion shifted fiber link for center wavelength at 1.55-μm. A Mach–Zehnder receiver is assumed.

The cause of this problem can be easily identified by introducing a time delay in the receiver demodulation signal. A time delay of 10 ps is introduced to the receiver and the corresponding data is shown in Fig. 8(b). The white spaces in the eye diagram appear now at longer spectral elements, which arrive at later times. Thus, we find that the group delay dispersion is more responsible for the deterioration of the signal than the phase error. A continuous phase variation results only in either time delay or group delay dispersion, but does not make the discrete phase coding undetectable. In conclusion, the problems associated with dispersion is not a consequence of using the FD-DPSK scheme, but of using broad bandwidth, which is the same for an ASK scheme or any other OTDM scheme.

We can reduce the effect of dispersion by use of DS fiber. In DS fiber, dispersion is minimized at 1.55 μm so that $b_2 = 0$ and the effect from b_3 is not negligible. Taking a typical value of 0.075 ps/nm^2· km for S_0 [17], we show in Fig. 8(c) that transmission of an FD-DPSK signal over 1000 km is not limited by the dispersion in DS fiber, in the case of 7 bit spectral data. However, transmission of broader spectral data will be limited by the group delay dispersion effect: Using the

same criterion as for clock jitter, i.e., $|\frac{d\beta}{d\omega}| < 25$ ps, we find that transmission of 500-bit data occupying 5-THz bandwidth will be limited to fiber links shorter than 1 km.

VI. Conclusions

The authors introduce a novel *frequency-domain differential phase shift keying* for use in femtosecond spectral modulation systems. In contrast to a traditional coherent optical communication system, FD-DPSK requires neither a reference phase nor a local oscillator for detection. The analysis of FD-DPSK detection demonstrates feasibility of the detection and a noise-robustness in a simple coherent optical communication system.

We propose *receiver designs* capable of OTDM demultiplexing and FD-DPSK demodulation simultaneously. These receivers consist of either a Mach–Zehnder interferometer and a pair of electrooptic phase modulators, or a Sagnac loop interferometer and a traveling-wave electrooptic phase modulator. The operation schemes of these receivers make use of novel ideas of a wavelength shift and a time gate with electrooptic linear phase variation only within a OTDM slot of interest. Modeling the receivers by computer analysis, we demonstrate how the Mach–Zehnder and Sagnac receivers demodulate the FD-DPSK signal. We also compare the detectability of signals transmitted through an extremely noisy system by the proposed FD-DPSK technique with that by a comparable ASK and direct detection technique. Our simulation study suggests that an FD-DPSK signal demodulated by a Mach–Zehnder receiver gives a better performance in noise reduction than the ASK technique. We also characterize the tradeoff between FD-DPSK transmission ultrabroad-band spectral data and the transmission distance, and show the limit is not set by the FD-DPSK scheme.

References

[1] A. M. Weiner, "Femtosecond optical pulse shaping and processing," *Prog. Quantum Electron.*, vol. 19, pp. 161–237, 1995, and references therein.

[2] A. Efimov, C. Schaffer, and D. H. Reitze, "Programmable shaping of ultrabroad bandwidth pulses from a Ti: Sapphire laser," *J. Opt. Soc. Amer. B*, vol. 12, no. 10, pp. 1968–1980, 1995.

[3] M. A. Dugan, J. X. Tull, and W. S. Warren, "High resolution, acousto-optic shaping of unamplified and amplified femtosecond laser pulses," *J. Opt. Soc. Amer. B*, vol. 14, no. 9, pp. 2348–2358, 1997.

[4] R. A. Griffin, D. D. Sampson, and D. A. Jackson, "Coherence coding for photonic code-division multiple access networks," *J. Lightwave Technol.*, vol. 13, pp. 1826–1837, 1995.

[5] M. Kavehrad and D. Zaccarin, "Optical code-division-multiplexed systems based on spectral encoding of noncoherent sources," *J. Lightwave Technol.*, vol. 13, pp. 534–545, Mar. 1995.

[6] E. A. De Souza, M. C. Nuss, W. H. Knox, and D. A. B. Miller, "Wavelength-division multiplexing with femtosecond pulses," *Opt. Lett.*, vol. 20, pp. 1166–1168, 1995.

[7] J.-K. Rhee, H. Kobayashi, and W. S. Warren, "Frequency-domain differential phase shift keying in femtosecond spread-time WDM/TDM systems," in *Proc. 1996 Conf. Inform. Sci. Syst.*, Princeton Univ., Princeton, NJ, 1996, vol. 2, pp. 1107–1112.

[8] C. W. Hillegas, J. X. Tull, D. Goswami, D. Strickland, and W. S. Warren, "Femtosecond laser pulse shaping by use of microsecond radio-frequency pulses," *Opt. Lett.*, vol. 19, pp. 737–739, 1994.

[9] M. Dugan, J. X. Tull, J.-K. Rhee, and W. S. Warren, "High-resolution ultrafast laser pulse shaping for quantum control and terabit per second communications," in *Tech. Dig. Ultrafast Phenomena*, 1996 OSA Optical Society of America, Washington DC, vol. 8, pp. 309–310, 1996.

[10] G. Einarsson, J. Strandberg, and I. T. Monroy, "Error probability evaluation of optical systems distributed by phase noise and additive noise," *J. Lightwave Technol.*, vol. 13, pp. 1847–1852, Sept. 1995.

[11] C. P. Kaiser, M. Shafi, and P. J. Smith, "Analysis methods for optical heterodyne DPSK receivers corrupted by laser phase noise," *J. Lightwave Technol.*, vol. 11, pp. 1820–1830, Nov. 1993.

[12] I. P. Kaminow *et al.*, "A wideband all-optical WDM network," *IEEE J. Select. Areas Commun.*, vol. 14, pp. 780–799, June 1996.

[13] J. K. Lucek and K. Smith, "All-optical signal regenerator," *Opt. Lett.*, vol. 18, no. 15, pp. 1226–1228, 1993.

[14] L. E. Adams, E. S. Kintzer, and J. G. Fujimoto, "Performance and scalability of an all-optical clock recovery figure eight laser," *IEEE Photon. Technol. Lett.*, vol. 8, pp. 55–57, Jan. 1996.

[15] O. Kamatani and S. Kawanishi, "Ultrahigh-speed clock recovery with phase lock loop based on four-wave mixing in a traveling-wave laser diode amplifier," *J. Lightwave Technol.*, vol. 14, pp. 1757–1767, Aug. 1996.

[16] J. Salz, "Coherent lightwave communications," *AT&T Tech. J.*, vol. 64, no. 10, pp. 2153–2209, 1985.

[17] Corning Product Information PI1043, *Corning SMF/DS Single-Mode Dispersion-Shifted Optical Fiber*, Corning Incorporated, Corning, NY, 1994.

June-Koo Rhee, photograph and biography not available at the time of publication.

Hisashi Kobayashi (S'66–M'68–SM'76–F'77) received the B.E. and M.E. degrees from the University of Tokyo, Tokyo, Japan, in 1961 and 1963, respectively, and the Ph.D. degree from Princeton University, Princeton, NJ, in 1967, all in electrical engineering.

Prior to coming to the United States, he worked at Toshiba Electric Co., Kawasaki, Japan, as a Radar System Designer from 1963 to 1965. He spent 19 years (1967–1986) with the IBM Research Division and held a number of technical management positions, including Senior Manager of Systems Analysis and Algorithms (1974–1980); Department Manager of VLSI Design (1981–1982); and the Founding Director of the IBM Tokyo Research Laoratory (1982–1986). He also held visiting professorships at UCLA (1969–1970), University of Hawaii, Honolulu, (1975), Stanford University, Stanford, CA, (1976), Technical University of Darmstadt, Germany (1979–1980), Free University of Brussels (1980), and University of Tokyo, Japan (1991–1992). In 1986 he joined the faculty of Princeton University as Dean of Engineering and Applied Science (1986–1991), and as the Sherman Fairchild Professor of Electrical Engineering and Computer Science (1986 to present). His past technical contributions include the invention of the PRML (partial-response coding, maximum-likelihood decoding) scheme which is now widely used in high-density digital recording. His current research interest includes: 1) performance analysis of ATM, optical, and wireless networks; 2) advanced coding and modulation schemes for digital communications and recording; and 3) teletraffic theory. He is the author of *Modeling and Analysis: An Introduction to System Performance Evaluation Methodology* (Reading, PA: Addison Wesley, 1978), and has published more than 130 technical papers and holds nine US patents. At Princeton University, he regularly teaches communication networks and digital communications and is currently preparing textbooks on these subjects.

Dr. Kobayashi is the recipient of the Humboldt Prize from Germany (1979), IFIP (International Federatiuon of Information Processing)'s Silver Core Award (1980); and IBM Outstanding Contribution Awards (1975 and 1984). He was elected a Member of the Engineering Academy of Japan (1992). He has served as a Scientific Advisor for many organizations, including NASA (Washington, DC), SRI International (Menlo Park, CA), the Institute of Systems Science (Singapore); and the Advanced Systems Institute (British Columbia, Canada).

Warren S. Warren, photograph and biography not available at the time of publication.